Coulomb Memory Signatures in the Excitonic Optical Stark Effect

C. Sieh, T. Meier, F. Jahnke, A. Knorr, and S. W. Koch
Department of Physics and Material Sciences Center, Philipps University, Renthof 5, D-35032 Marburg, Germany

P. Brick, M. Hübner, C. Ell, J. Prineas, G. Khitrova, and H. M. Gibbs
Optical Sciences Center, University of Arizona, Tucson, Arizona 85712
(Received 4 November 1998)

Differential absorption spectra of high-quality InGaAs quantum wells are presented for various pump detunings and polarization configurations. For low intensity pump pulses tuned well below the exciton a redshift is observed for opposite circularly polarized probe pulses. Microscopic calculations show that this redshift originates from memory effects in the Coulomb-induced excitonic correlations. [S0031-9007(99)08917-6]

PACS numbers: 71.35.Cc, 42.50.Md, 78.66.–w

Since the discovery of the optical Stark effect in semiconductors [1–7] the understanding of ultrafast nonlinear optical effects in excitonic systems has been—and still is—of fundamental interest. Recently, it has been demonstrated that for a proper understanding of nonlinear experiments like four-wave mixing and pump probe, even in the low-density $\chi^{(3)}$ limit (third order in the optical field), Coulomb-induced many-body carrier correlations need to be considered [8–16]. In the coherent $\chi^{(3)}$ limit these correlations manifest themselves in the contributions of bound and unbound two-exciton states to the optical response [9,10,14].

For the theoretical analysis of correlation effects different schemes have been developed: If plasma excitation dominates, bound exciton complexes are of less importance and the correlation effects can be treated in second Born approximation in the Markov limit [14,16]. For relatively low, resonant excitation conditions where biexcitonic effects and memory effects [17–21] need to be considered explicitly, it is advantageous to use the dynamics controlled truncation scheme [9], which includes in a natural way the dynamics of the higher-order Coulomb correlations.

In this Letter, we investigate configurations where we expect higher-order Coulomb correlation effects to be significant. For this purpose we measure and compute differential absorption spectra of high-quality InGaAs quantum wells with spectrally very narrow exciton linewidth. The experiments are performed using various detunings and polarizations of the pump and probe pulses (cocircularly $\sigma^+\sigma^+$, opposite circularly $\sigma^+\sigma^-$, linear parallel xx, and linear perpendicular xy). The linear absorption spectra are dominated by a heavy-hole exciton resonance with a spectrally very narrow linewidth of 0.56 meV, energetically separated well below all other exciton resonances [22]. Hence, we can perform pump-probe experiments that are influenced only by heavy-hole exciton states and its higher-order correlations [23]. The structure, consisting of thirty 8.5 nm thin $In_{0.04}Ga_{0.96}As$ quantum wells, was grown by molecular beam epitaxy on a semi-insulating GaAs substrate, providing the unique opportunity to perform experiments in transmission geometry without removal of the substrate, which usually would result in degraded sample quality. Both pump and probe pulses were generated by an actively mode-locked Ti:sapphire laser. The spectrally broad 100 fs short pulses were used for probing the heavy-hole hh-exciton resonance while pumping simultaneously with a pulse spectrally narrowed by an external pulse shaper. The spectral width of the pump pulses was reduced to about 2.3 meV resulting in a temporal width of 1.5 ps. The spectrally resolved pump-probe experiments were performed in transmission geometry at helium temperatures. The signal was detected with a diode array behind a spectrograph. The laser pulses were focused down to a spot diameter of 100 μm. The weak probe pulse energy of 0.1 pJ, with a pulse repetition rate of 80 MHz, resulted in an average intensity of 0.1 W/cm^2 while the pump pulses had an energy of 125 pJ corresponding to an average intensity of 127 W/cm^2.

Our most exciting result, and—as we will show below—a clear signature of Coulombic memory effects, is that for off-resonant excitation (4.5 meV below the exciton), we clearly see in Fig. 1(d) a *redshift* if the pump and probe pulses are opposite circularly polarized, whereas a *blueshift* is observed for $\sigma^+\sigma^+$, xx, and xy polarized pump and probe pulses. The 4.5 meV detuning is considerably larger than the biexciton binding energy, the inhomogeneous linewidth, as well as the spectral width of the pump pulse, ensuring that the excitation is off-resonant. Varying the detuning towards smaller and larger values does not change the qualitative behavior. Also for resonant excitation, besides bleaching of the exciton resonance, clear signatures of excited state absorption due to unbound two-exciton complexes are observed for both co- and opposite circular polarized pump and probe pulses. Additionally, for $\sigma^+\sigma^-$ excitation biexciton-induced absorption features appear energetically below the exciton resonance.

 0031-9007/99/82(15)/3112(4)$15.00

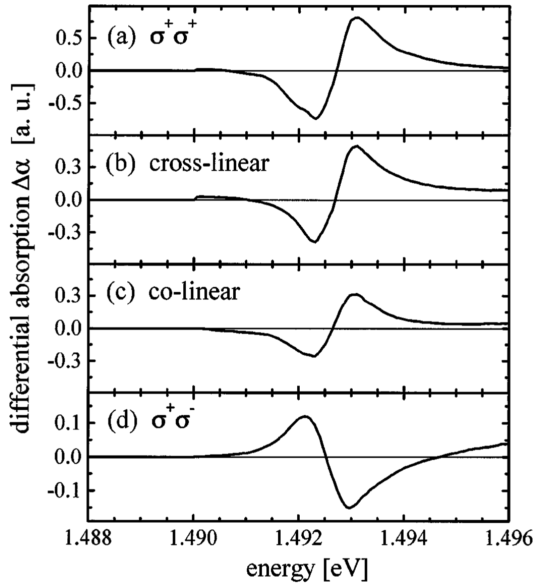

FIG. 1. Experimental differential absorption spectra at $\tau = 0$ ps for off-resonant excitation (4.5 meV below the 1s hh-exciton resonance). (a) cocircularly, (b) crosslinearly, (c) colinearly, and (d) opposite circularly polarized pump and probe pulses.

To theoretically model these effects we compute the optical response in the coherent $\chi^{(3)}$ limit without further approximations [9,10]. We numerically solve the equations, both for a fully two-dimensional model of the quantum-well structure [16] and for a simplified, quasi-one-dimensional system [24]. In the one-dimensional tight-binding model electron and heavy-hole couplings of 8 and 0.8 meV, respectively, between neighboring sites are used. The two spin-degenerate electron and heavy-holes bands, respectively, are considered and we use the usual circularly polarized dipole matrix elements describing the optical transitions between these bands [14]. The Coulomb Hamiltonian H_C has the form

$$H_C = \frac{1}{2} \sum_{ijcvc'v'} (a_i^{c'+} a_i^{c'} - a_i^{v'+} a_i^{v'}) \times V_{ij} (a_j^{c+} a_j^{c} - a_j^{v+} a_j^{v}),$$

where, i and j refer to real-space sites, and c (v) label the conduction (valence) bands. a_i^{c+} (a_j^c) creates (destroys) an electron at site i (j) in band c, and a_i^{v+} (a_j^v) creates (destroys) a hole at site i (j) in band v. V_{ij} describes the monopole-monopole Coulomb interactions between particles at sites i and j. The Coulomb interaction V_{ij} is given by a regularized potential:

$$V_{ij} = U_0 \frac{d}{|i - j|d + a_0},$$

where d is the distance between the sites and U_0 and a_0 are parameters characterizing the strength of the interaction and the spatial variation. In our numerical study we use $U_0 = 8$ meV and $a_0/d = 0.5$ [25]. Whereas the numerics for the two-dimensional system is extremely involved and time consuming the one-dimensional model allows a more detailed analysis. For example, we identify three types of optical nonlinearities: the total differential absorption signal is the sum of a Pauli blocking term and Coulomb-induced many-body nonlinearities, which can further be separated into a first-order term and higher-order correlations [14,26].

We present numerical results both for the one-dimensional model and for our two-dimensional quantum-well system. First we investigate the situation where the pump pulse is tuned 4.5 meV below the exciton resonance. Figures 2(a)–2(d) display the theoretical results for $\sigma^+\sigma^+$ and $\sigma^+\sigma^-$ excitation. In agreement with the experiment (see Fig. 1), in $\sigma^+\sigma^+$ configuration, see Figs. 2(a) and 2(c) [and also for xy and xx excitation (not shown)], the differential absorption corresponds to a blueshift whereas for $\sigma^+\sigma^-$ [Figs. 2(b) and 2(d)] there is a redshift.

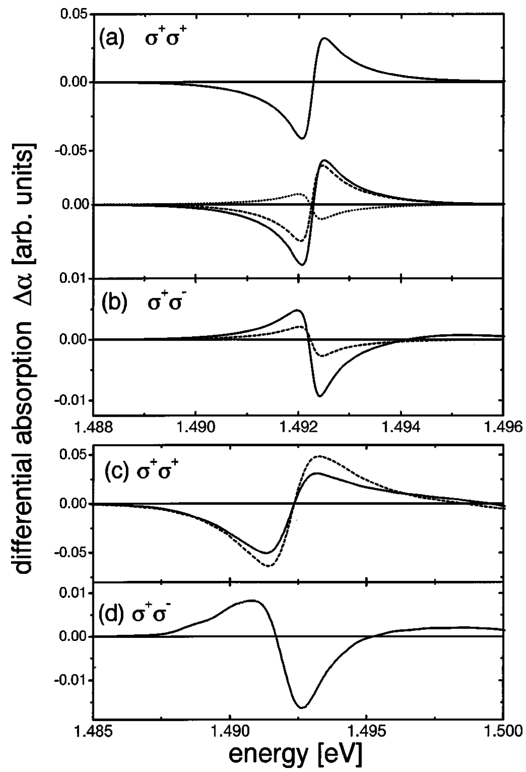

FIG. 2. Calculated differential absorption spectra for excitation 4.5 meV below the exciton and $\tau = 0$ ps. (a) One-dimensional model, cocircularly polarized pump and probe pulses ($\sigma^+\sigma^+$), the lower panel shows the three contributions to the signal (solid line: Pauli blocking; dashed line: first-order Coulomb; and dotted line: Coulomb correlation). (b) One-dimensional model, opposite circularly polarized pump and probe pulses ($\sigma^+\sigma^-$). The dashed line represents the result of a calculation without biexcitons, as discussed in the text. (c) same as (a) and (d) same as (b), respectively, but for the full two-dimensional quantum-well model. The dashed line in (c) displays the result of a Hartree-Fock calculation neglecting Coulomb correlations.

Note that for $\sigma^+\sigma^-$ excitation both the Pauli blocking and the first-order Coulomb-induced nonlinearity, i.e., the Hartree-Fock contribution, vanish identically, because neither one of these terms leads to a coupling among the subspaces of different spin states within $\chi^{(3)}$ [8,14]. Thus in this case the total signal is purely induced by Coulomb correlations.

The physical origin of the redshift can be further analyzed by looking at the individual contributions to the signal. We find that for $\sigma^+\sigma^+$ polarization for strong detuning below the exciton the Pauli blocking and the first-order Coulomb term always induce a blueshift, whereas the Coulomb correlations always correspond to a redshift. The fact that also for $\sigma^+\sigma^+$ excitation, where no bound biexcitons are excited, the correlation term alone still corresponds to a redshift demonstrates that this shift is not directly related to the existence of a bound biexciton.

To support this conclusion we performed additional calculations of the differential absorption spectra in $\sigma^+\sigma^-$ configuration. To eliminate the bound biexciton contribution also for $\sigma^+\sigma^-$ excitation we artificially dropped the six terms containing the attractive and repulsive Coulomb terms for two electrons and two holes from the homogeneous part of the equation of motion for the two-exciton amplitude B [see Eq. (2.7) of Ref. [14]]. In this case, also for $\sigma^+\sigma^-$ excitation no bound biexcitons exist, but the result displayed in Fig. 2(b) shows that signal amplitude is somewhat reduced, the redshift, however, clearly persists. The same artificial calculations performed for $\sigma^+\sigma^+$ excitation (not shown in figure) where no biexciton is excited yield a similar result. The signal amplitude of the correlation term is reduced, but its redshift persists. This means that for the occurrence of the redshift the exact structure of the two-exciton states seems to be unimportant. However, calculations where the Coulomb correlations are treated in second Born and Markov approximation did not yield a redshift. Hence, the redshift is inherently a non-Markovian signature and thus a consequence of Coulomb-memory effects.

To verify the validity of the theoretical analysis also the case of resonant excitation has been investigated. The measured differential absorption spectra for resonant excitation and zero time delay between pump and probe pulses, Fig. 3, show pronounced bleaching of the exciton resonance. Increased absorption appears energetically above the exciton for cocircular and also below for opposite circular pump-probe polarization configurations.

Numerical results for the resonant excitation considering $\sigma^+\sigma^+$ and $\sigma^+\sigma^-$ excitation are presented in Fig. 4 showing very good qualitative agreement with the experimental data in Fig. 3. For $\sigma^+\sigma^+$ excitation besides the total differential absorption also the three individual contributions are displayed; see Fig. 4(a). It is shown that the Pauli-blocking induces bleaching of the exciton and that it is very small compared to the Coulomb-induced nonlinearities, as is expected for resonant excitation [14,26].

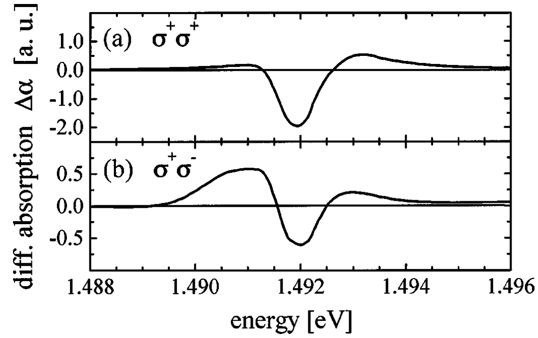

FIG. 3. Experimental differential absorption spectra at $\tau = 0$ ps for resonant excitation. (a) Cocircularly, and (b) opposite circularly polarized pump and probe pulses.

The first-order and correlation Coulomb-induced nonlinearities are mainly dispersive in shape corresponding to a blue- and redshift, respectively. The total signal is given by the sum of all three terms. By adding up the two Coulomb-induced nonlinearities their dispersive character

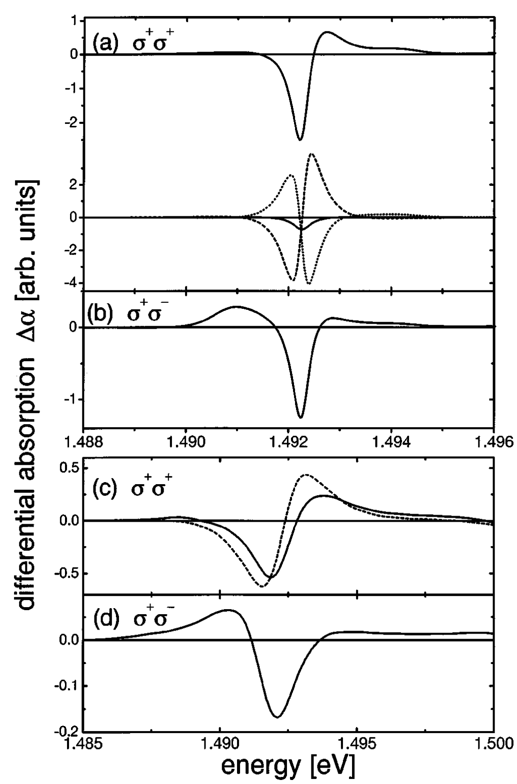

FIG. 4. Calculated differential absorption spectra for resonant excitation at the exciton and $\tau = 0$ ps. (a) One-dimensional model, cocircularly polarized pump and probe pulses ($\sigma^+\sigma^+$), the lower panel shows the three contributions to the signal (solid: Pauli-blocking, dashed: first-order Coulomb, and dotted: Coulomb correlation). (b) One-dimensional model, opposite circularly polarized pump and probe pulses ($\sigma^+\sigma^-$). (c) same as (a) and (d) same as (b), respectively, but for the full two-dimensional quantum-well model. The dashed line in (c) displays the result of a Hartree-Fock calculation neglecting Coulomb correlations.

at the exciton resonance disappears due to strong cancellations among them. The resulting signal shows bleaching at the exciton resonance, which is dominated by the Coulomb-induced nonlinearities (note that the amplitude of the bleaching at the exciton is much larger than the Pauli-blocking contribution) and excited state absorption at higher energies induced by unbound two exciton states. Figures 4(b) and 4(d) show the corresponding differential absorption spectrum for $\sigma^+\sigma^-$ polarizations. Around and above the exciton resonance it is very similar to the spectrum obtained for $\sigma^+\sigma^+$. In addition, a clear positive excited state absorption feature appears below the exciton resulting from the biexciton that is excited in this configuration.

So far, to the best of our knowledge, for large detuning (the detuning should be considerably larger than the biexciton binding energy, the inhomogeneous linewidths, and the spectral width of the pump pulse) below the exciton resonance all experiments performed on direct semiconductors report a blueshift [1,2,27–29]. A redshift has been observed only in CuCl, which has an extremely large biexciton binding energy, in a small spectral window when the pump pulse is tuned slightly below the exciton to biexciton transition using parallel linearly polarized pump and probe pulses [30]. Theoretically this redshift was related to the existence of a bound biexciton [31]. However, for increased detuning to lower frequencies and for parallel linear polarized pulses one always recovers the blueshift of the "dressed atom picture" [31]. In contrast, the redshift observed here for large detuning using opposite circularly polarized pulses is induced by Coulomb correlations, but is not directly related to the existence of a bound biexciton and has its origin in Coulomb-memory effects. The Coulomb-memory signatures discussed here induce spectral characteristics at the energy of the fundamental 1s hh exciton. They are thus different from the memory-effects reported recently in Ref. [32] which involved excitation high above the band gap, and the buildup of the free-carrier Coulomb screening.

The Marburg part of this work is supported by the Deutsche Forschungsgemeinschaft (DFG) through the Sonderforschungsbereich 383, the Quantenkohärenz Schwerpunkt, the Heisenberg and Leibniz programs, and by the HLRZ Jülich through grants for extended CPU time on their supercomputer systems. The Tucson part acknowledges the support by NSF (AMOP and LWT), AFOSR/DARPA, JSOP (AFOSR and ARO), and COEDIP. C. E. thanks the DFG for partial support.

[1] D. Fröhlich, A. Nöthe, and K. Reimann, Phys. Rev. Lett. **55**, 1335 (1985).
[2] A. Mysyrowicz *et al.*, Phys. Rev. Lett. **56**, 2748 (1986).
[3] A. Von Lehmen *et al.*, Opt. Lett. **11**, 609 (1986).
[4] S. Schmitt-Rink and D. S. Chemla, Phys. Rev. Lett. **57**, 2752 (1986); S. Schmitt-Rink, D. S. Chemla, and H. Haug, Phys. Rev. B **37**, 941 (1988).
[5] B. Fluegel *et al.*, Phys. Rev. Lett. **59**, 2588 (1987).
[6] W. Schäfer, Adv. Solid State Phys. **28**, 63 (1988).
[7] C. Ell *et al.*, Phys. Rev. Lett. **62**, 304 (1989).
[8] H. Wang *et al.*, Phys. Rev. Lett. **71**, 1261 (1993).
[9] V. M. Axt and A. Stahl, Z. Phys. B **93**, 195 (1994); **93**, 205 (1994).
[10] M. Lindberg *et al.*, Phys. Rev. B **50**, 18 060 (1994).
[11] Th. Östreich, K. Schönhammer, and L. J. Sham, Phys. Rev. Lett. **74**, 4698 (1995).
[12] T. Rappen *et al.*, Phys. Rev. B **49**, 10 774 (1994).
[13] D. S. Chemla *et al.*, Phys. Rev. B **50**, 8439 (1994).
[14] W. Schäfer *et al.*, Phys. Rev. B **53**, 16 429 (1996).
[15] P. Kner *et al.*, Phys. Rev. Lett. **78**, 1319 (1997).
[16] F. Jahnke *et al.*, Phys. Rev. Lett. **77**, 5257 (1996).
[17] L. Bànyai *et al.*, Phys. Rev. Lett. **75**, 2188 (1995).
[18] H. Haug and A. P. Jauho, *Quantum Kinetics in Transport and Optics of Semiconductors* (Springer, Berlin, 1996).
[19] S. Bar-Ad *et al.*, Phys. Rev. Lett. **77**, 3177 (1996).
[20] C. Fürst *et al.*, Phys. Rev. Lett. **78**, 3733 (1997).
[21] M. U. Wehner *et al.*, Phys. Rev. Lett. **80**, 1992 (1998).
[22] C. Ell *et al.*, Phys. Rev. Lett. **80**, 4795 (1998).
[23] It is a crucial point in the present experiments that only heavy holes and no light holes are excited. If light holes would contribute significantly to the optical response, then also for $\sigma^+\sigma^-$ excitation and strong detuning below the exciton one gets a blueshift [29]. This is nothing but the simple "dressed atom" blueshift which stems from the fact that a light-hole exciton excited with a σ^+ pulse involves the same electron band as the heavy hole exciton excited with a σ^- pulse.
[24] D. Brinkmann *et al.*, Phys. Status Solidi (b) **206**, 493 (1998).
[25] The parameters chosen in the model result in an exciton binding energy of 8 meV and a biexciton binding energy of 1.4 meV. Homogeneous broadening is introduced phenomenologically through decay rates of $\gamma_p = (3\ \text{ps})^{-1}$ for single excitons and $\gamma_B = (1.5\ \text{ps})^{-1}$ for two excitons. The pump pulse has a Gaussian envelope with 1.18 ps (full width at half maximum) duration for the pulse intensity. These values are close to the experimental situation. For numerical convenience in the two-dimensional calculations $\gamma_p = (0.6\ \text{ps})^{-1}$ and $\gamma_B = (0.3\ \text{ps})^{-1}$ is used.
[26] G. Bartels *et al.*, Phys. Rev. B **55**, 16 404 (1997).
[27] N. Peyghambarian *et al.*, Phys. Rev. Lett. **62**, 1185 (1989).
[28] W. H. Knox *et al.*, Phys. Rev. Lett. **62**, 1189 (1989).
[29] M. Joffre *et al.*, Phys. Rev. Lett. **62**, 74 (1989).
[30] D. Hulin and M. Joffre, Phys. Rev. Lett. **65**, 3425 (1990).
[31] M. Combescot and R. Combescot, Phys. Rev. Lett. **61**, 117 (1988).
[32] L. Bànyai *et al.*, Phys. Rev. Lett. **81**, 882 (1998).